Ventricular wall granulations may help drain CSF in giant hydrocephalus

ONLINE SUPPLEMENT CONTAINING:

(1) Methodology and results for the MRI and PET from the woman described in the *Introduction*

(2) Diagram of a proposed CSF-resorption compensatory mechanism in chronic giant hydrocephalus (Fig S3)

(3) Supplemental Discussion

Methods for the study of the woman with hydrocephalus mentioned in the *Introduction*

A 44-year-old woman with chronic giant hydrocephalus and five healthy women of similar age without known neurological disorders and normal MRIs were studied after written informed consent for a project on the study of giant hydrocephalus, approved by the Ethics Committee of the University of Navarra Medical School, in accordance with the Helsinki Declaration for the study of human subjects.[1] Neurological and neuropsychological examinations, the latter using the Wechsler Adult Intelligence Scale-Revised, were completed.

MRI procedure

MRI was performed on a 3 T Siemens Trio system (Siemens Medical Solutions, Erlangen, Germany). T1-weighted structural images (Fig 1a, b) were acquired using a 3D magnetization prepared rapid gradient echo sequence, with imaging parameters: resolution=1x1x1.1mm^3, FOV= 240x256 mm^2, 160 sagittal slices, TR/TE/TI=2250/900/2.96 ms, flip angle= 9º, BW=230 Hz/pixel. The T2-weighted image (Fig 1c) was acquired using a 3D fast spin-echo with variable refocusing flip angle, with imaging parameters: resolution=0.98x0.98x1 mm^3, FOV= 224x256 mm^2, TR/TE=3200/530 ms, BW=435 Hz/pixel, 2 averages. The susceptibility-weighted image (Fig 1d) was acquired using a 3D gradient-echo sequence with flow compensation in three directions, with imaging parameters: resolution=0.72x0.72x16 mm^3, FOV= 240x320 mm^2, TR/TE=28/20 ms, flip angle=15º, BW=120 Hz/pixel.[2]

Perfusion-weighted images were obtained using the pulse arterial spin labelling (PASL) technique. The PASL sequence consisted of a modified version of the flow-sensitive alternating inversion recovery technique with a saturation pulse applied after the global or slice-selective inversion.[3] Label and control images were acquired using a 2D gradient-echo echo planar imaging sequence, with imaging parameters: in-plane resolution=4x4 mm^2, FOV= 256x256 mm^2, slice thickness = 6 mm, 16 axial slices, TR/TE=3500/17 ms, BW=2895 Hz/pixel. Cerebral blood flow (CBF) values were obtained in the volumes of white and gray matter indicated by the regions of interest on Fig S1.

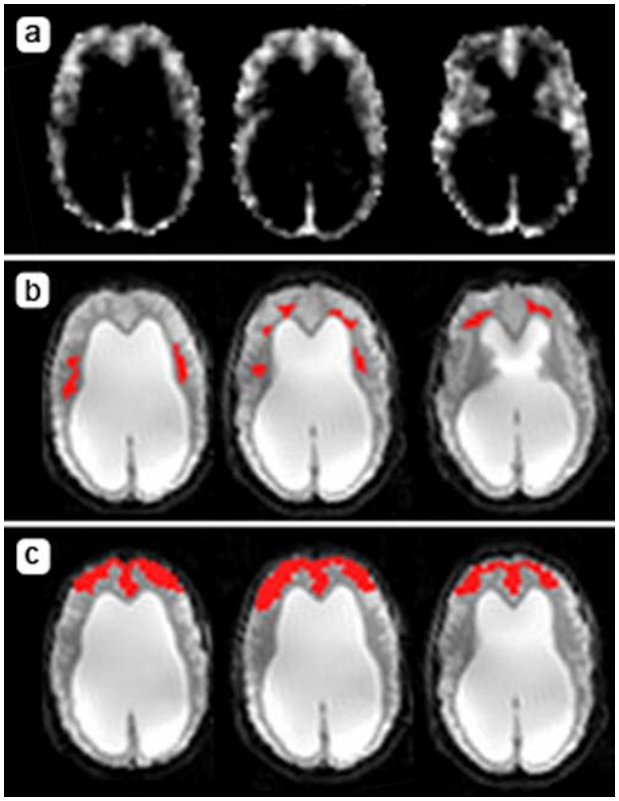

Figure S1. rCBF map from a 44-year-old woman with giant hydrocephalus. **a**, Three slices of the regional cerebral blood flow (rCBF) map, obtained with magnetic resonance imaging by means of the pulse arterial spin labelling (PASL) technique. **b**, **c**, Location of the tissue sampled to measure white matter (**b**) and gray matter (**c**) perfusion.

Study of brain metabolism with FDG PET

Brain metabolism was obtained by means of ^{18}F deoxyglucose positron emission tomography (FDG PET). Scanning was performed with an ECAT EXACT HR+ (Siemens/CTI, Knoxville, TN), 40 minutes after the intravenous injection of 14.4 mCi of ^{18}FDG, obtaining 63 simultaneous parallel planes over a 15.2 cm axial field of view. The tomographic resolution was 4.5 mm. Transmission scanning was done prior to radiopharmaceutical injection using three ^{68}Ge rotating rod sources. The subject was positioned so that the entire intracranial volume, including the cerebellum, was included in the field of view. As in order to make the study more comfortable for the subject arterial sampling was not performed, relative activity values were obtained. For this purpose, the brain PET study of the subject and of five normal controls were co-registered with their own MRIs and

spatially normalized with SPM2 software (Wellcome Department of Imaging Neuroscience, University College of London) using the template of the Montreal Neurological Institute. Two procedures were then performed, a regional activity comparison and a determination of the global Standard Uptake Value for the entire brain.

Relative regional brain activity

To facilitate the anatomical identification of the structures included in the regions of interest (ROIs), the PET study was superimposed to the MRI study of the subject of interest (Fig 1f) and to a canonical MRI for the controls. The cortical regions of the hydrocephalic subject included only those with enough volume to avoid a partial-volume error. Given the marked distortion of the cortex in the woman with hydrocephalus, whose abnormality was rostral to the atretic Sylvian aqueduct, and the relative preservation of the cerebellum on her MRI (Fig 1b,c) the ROIs were normalized for activity using as reference the activity of the entire cerebellum of each subject. The normalized activity from the hydrocephalic woman in the ROIs outlined on Fig S2 was then compared to that from the five normal controls. Areas with abnormal activity were considered those in which the activity was outside two standard deviations of the activity in similar regions of the control group.

Global brain activity

To compare the activity of the entire brain of the subject of interest to corresponding activity in the brain of the controls, we used the following formula to estimate the global brain Standard Uptake Value (SUV) for each subject:

Global brain SUV=[Bq/cc] in whole brain VOI/(injected dose of ^{18}FDG/patient weight),

where Bq/cc are Bequerel units (a radioactivity scale) per cubic centimetre and VOI is *volume of interest*. To determine the whole brain VOI for each subject, we used their T1-weighted MRI images. First, cortical surface representations were obtained with BrainSuite 2.[4] White and grey matter was then segmented from CSF using a segmentation routine based on FUZZY C-means written in MATLAB. A mask of brain tissue (white and grey matter) was used to define the whole brain VOI. This VOI was placed on the co-registered PET image and the global brain SUV calculated for each subject. The SUV was considered abnormal in the subject of interest if it was outside two standard deviations of the mean SUV activity of the control group.

Figure S2. Regions of interest (ROIs) on an ^{18}FDG PET study from a woman with giant hydrocephalus and on a normalized study from five controls.

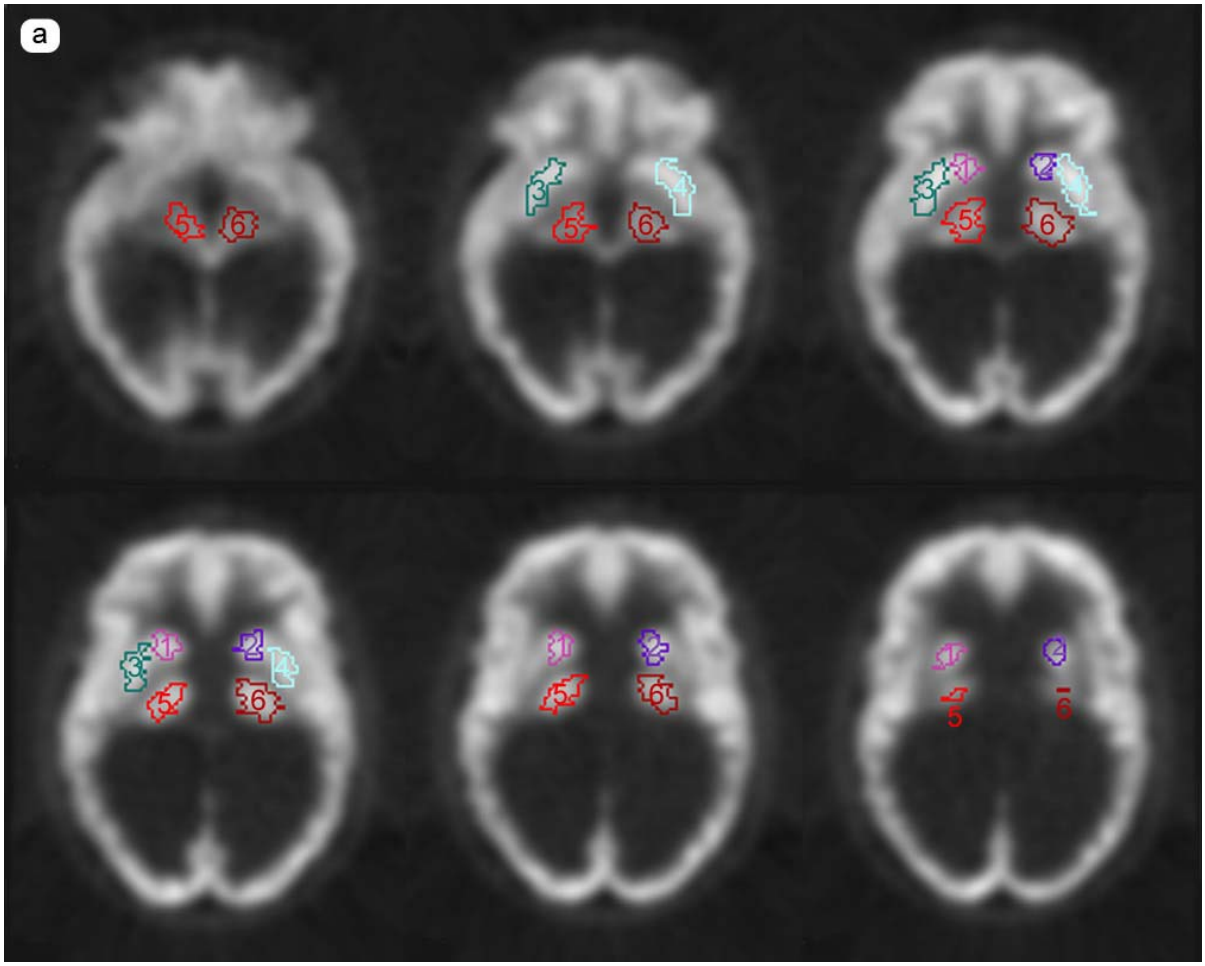

a, Subcortical ROIs for the woman with giant hydrocephalus.

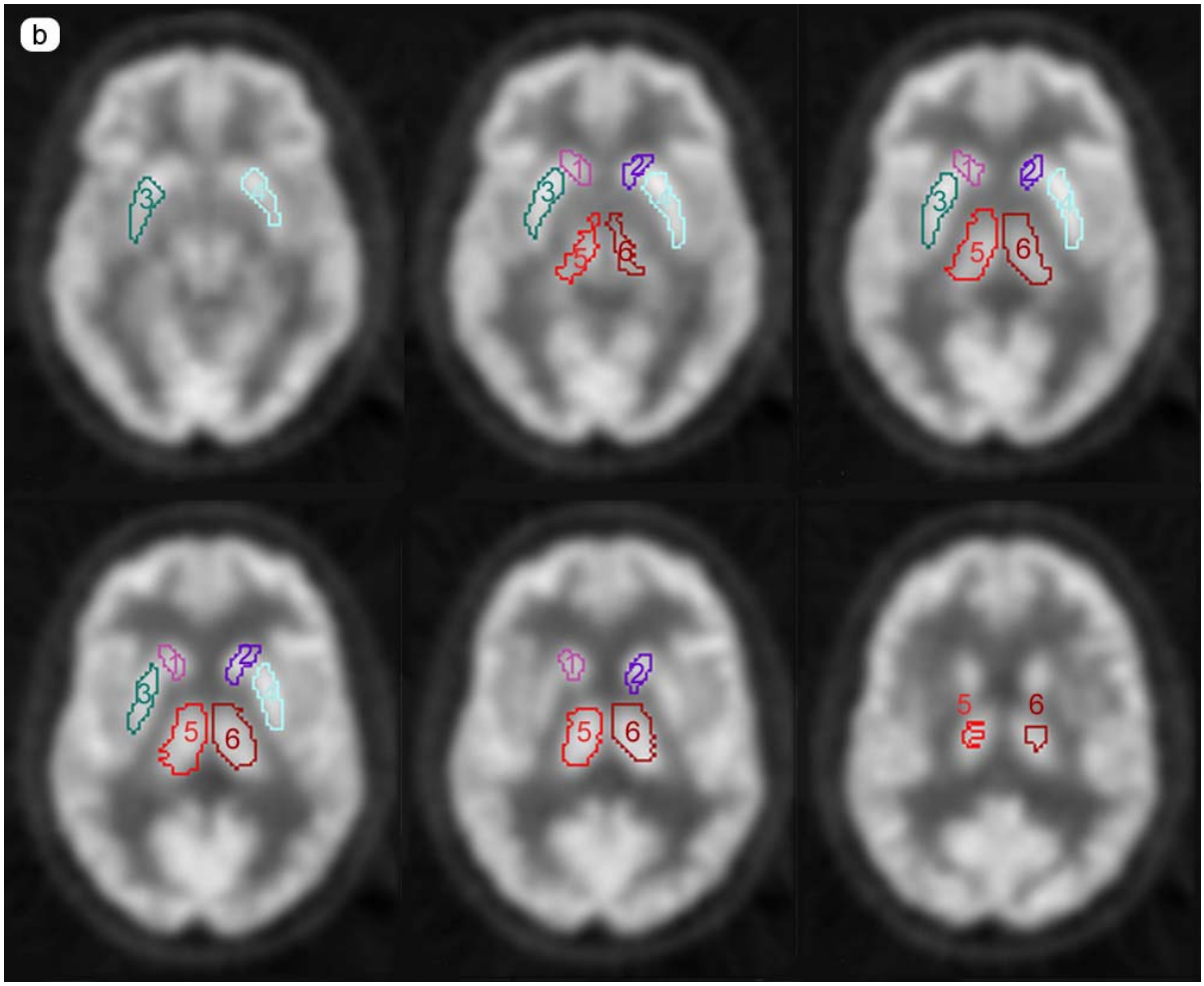

b, Subcortical ROIs for the controls.

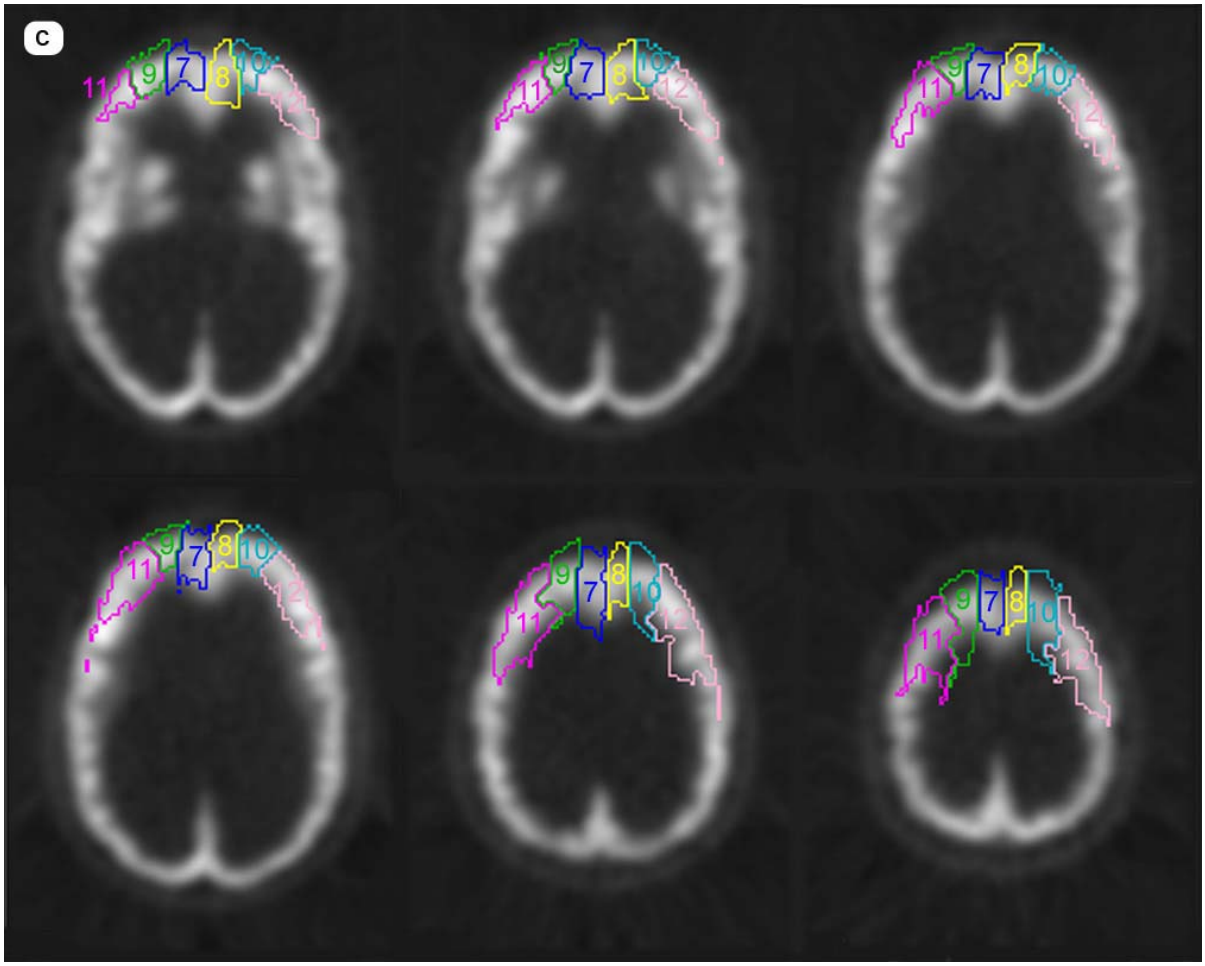

c, Cortical ROIs for the woman with giant hydrocephalus.

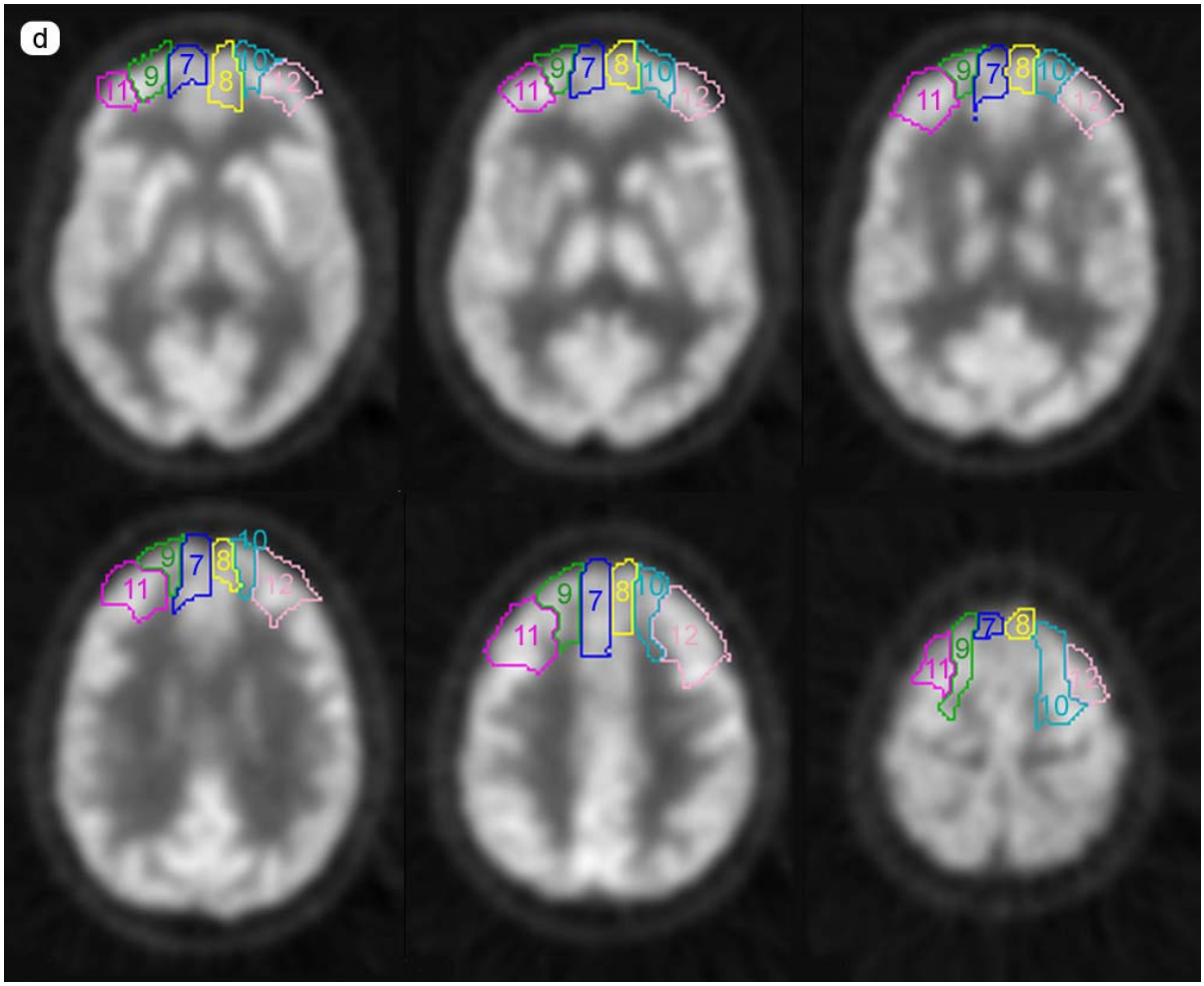

d, Cortical ROIs for the controls.

Findings in the woman with giant hydrocephalus described in the Introduction

In the 44-year old woman with chronic giant hydrocephalus mentioned in the Introduction, average regional perfusion values for the white matter and the gray matter regions outlined in Fig S1 were normal (see Table S1). Brain metabolism ratios for the regions outlined in Fig S2 were within the normal range (see Table S2), as was the global brain Standard Uptake Value (SUV in the subject with hydrocephalus = 3,720; mean SUV in the controls = 3,283 ± 0,645)

Table S1. **Normal brain rCBF in a 44-year-old woman with chronic giant hydrocephalus**

Region	**44-year-old woman**	**CASL 3T reference data** [5]	**[$^{15}OH_2$]PET reference data** [6]
White matter	20.02	22.4 ± 4.0	23.7 ± 3.8
Gray matter	54.03	49.5 ± 6.2	58.5 ± 9.9

rCBF = regional cerebral blood flow; CASL = continuous arterial spin labeling; PET = positron emission tomography

rCBF was calculated in the white matter and gray matter regions of interest displayed in Fig S1. All measurements (mean ± SD) are in mL/100g/min.

Table S2. Brain metabolism ratios for the regions outlined in Fig S2

Subcortical regions*	**		Hydrocephalic woman	Average (± SD) of 5 normal controls
1		R caudate	1.44	1.29 ± 0.07
2		L caudate	1.46	1.27 ± 0.10
3		R putamen	1.66	1.43 ± 0.10
4		L putamen	1.69	1.45 ± 0.13
5		R thalamus	1.19	1.21 ± 0.11
6		L thalamus	1.24	1.21 ± 0.11
Cortical regions				
7		Right superior frontal gyrus (medial)	1.19	1.15 ± 0.17
8		Left superior frontal gyrus (medial)	1.16	1.16 ± 0.16
9		Right superior frontal gyrus (lateral)	0.96	1.07 ± 0.14
10		Left superior frontal gyrus (lateral)	0.98	1.10 ± 0.15
11		Right middle frontal gyrus	1.30	1.16 ± 0.14
12		Left middle frontal gyrus	1.43	1.15 ± 0.14
		Average of the cortical regions	1.08	1.13 ± 0.13

* These numbers correspond to the regions numbered in Fig S2

** Colours correspond to the colour codes of the regions in Fig S2

Figure S3. Diagram of the normal adult human CSF circulation (a, c) and a proposed CSF-resorption mechanism in giant chronic hydrocephalus (b, d), based on the autopsy findings in the 48-year-old man described in the text. Images represent the medial view of a hemisphere (**a**, **b**) and coronal sections of both hemispheres at a pre-thalamic level (**c**, **d**).

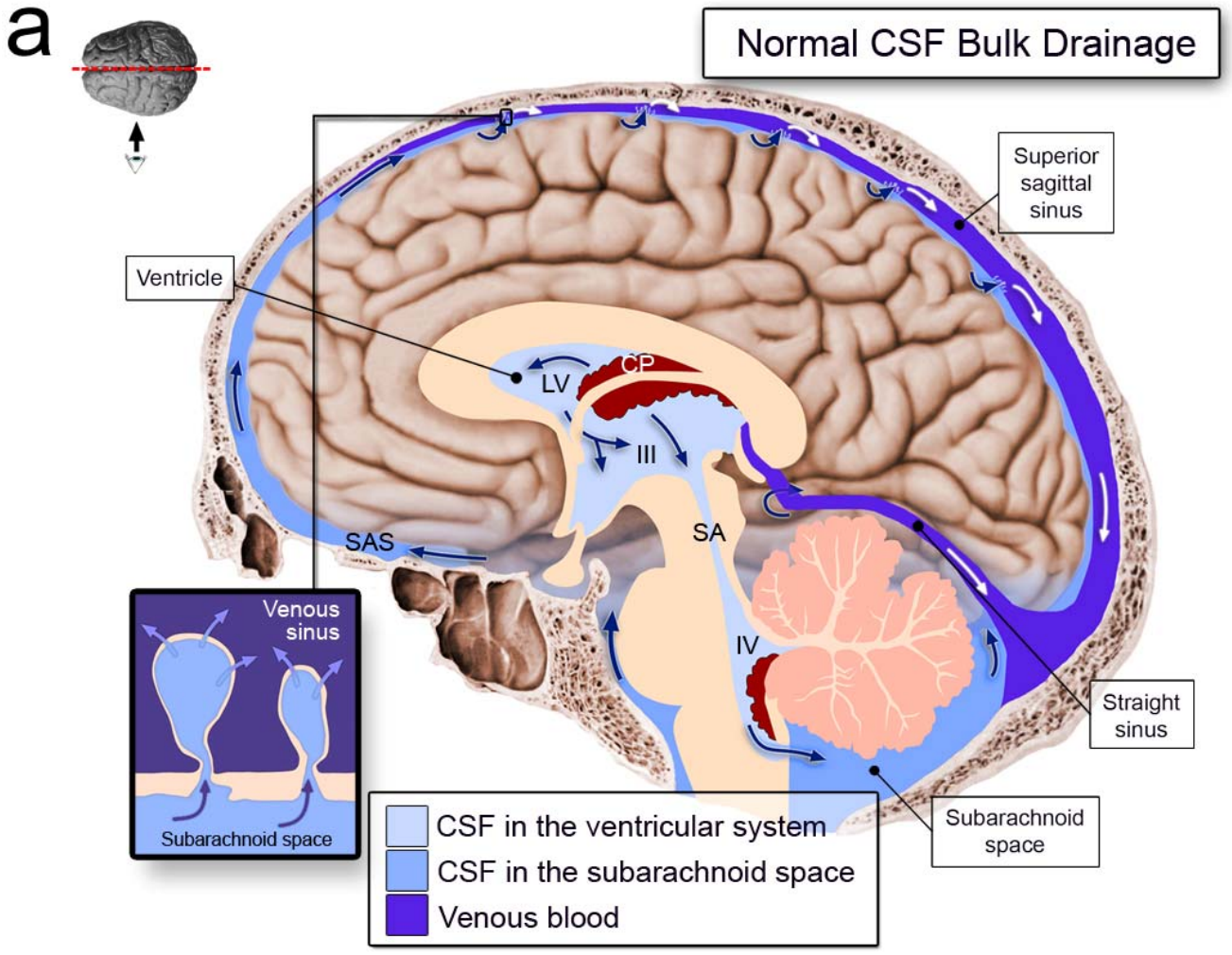

S1a. Normal CSF circulation *(medial view of the brain).* Cerebrospinal fluid (CSF) is normally secreted by the choroid plexus (CP), mostly in the lateral ventricles (LV). It drains through the third ventricle (III), the Sylvian aqueduct (SA) and the fourth ventricle (IV), exiting the ventricular system through the foramina of Luschka and Magendie, which communicate the fourth ventricle with the subarachnoid space (SAS) around the brain. In the SAS the CSF moves toward the large venous sinuses located in the fibrous layer that separates the brain from the bone of the skull. A valve-like system, constituted by the Pacchionian granulations (inset), separates the CSF from the blood in the venous sinuses, while permitting CSF to drain into the venous system.

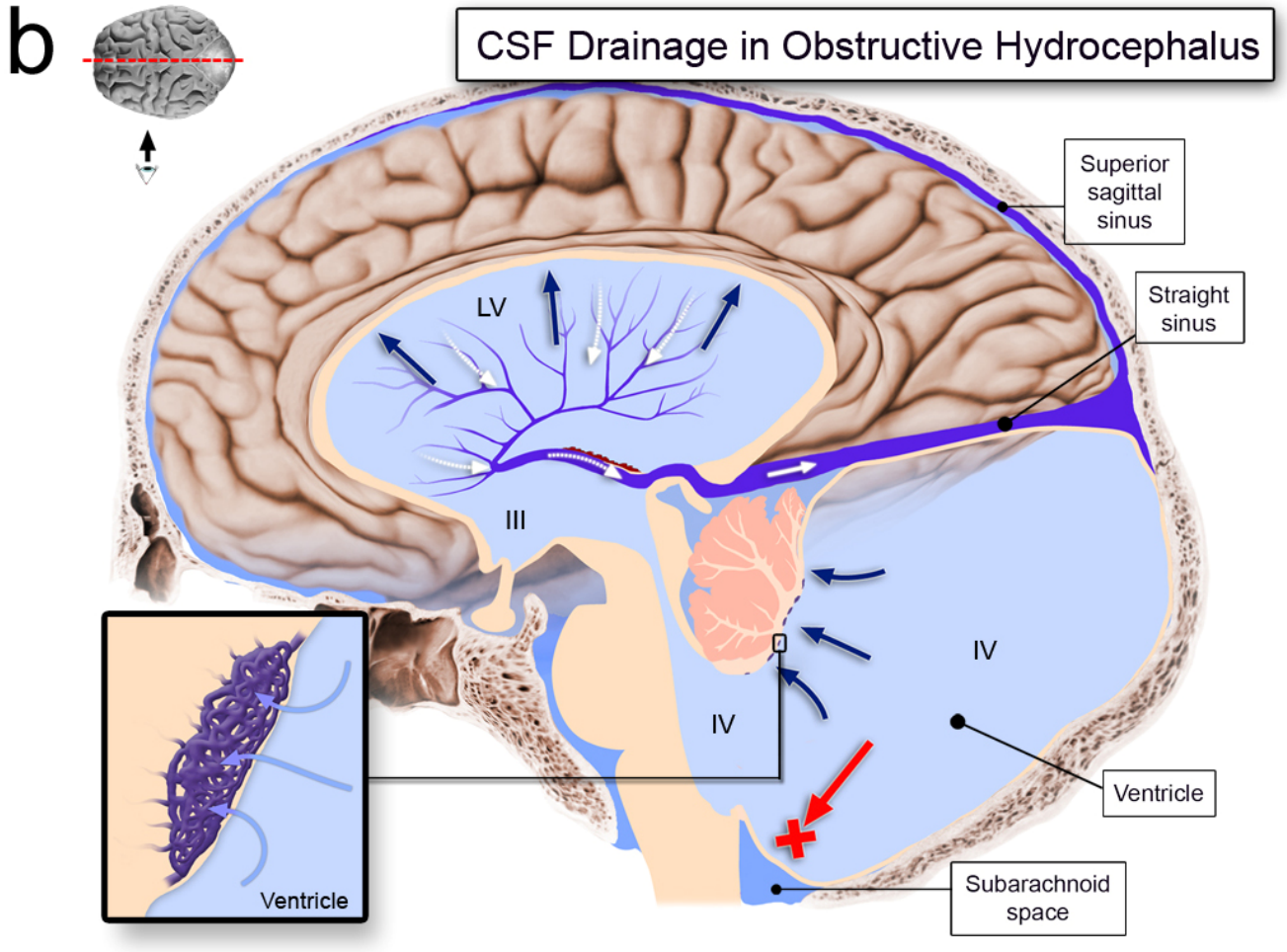

S3b. Hypothesized CSF flow in subjects with compensated giant hydrocephalus *(medial view of the brain).* Compare with Figs 2 and S3b. Obstruction of ventricular outflow, in the case of the patient with Dandy Walker syndrome due to lack of perforation of the foramina of Luschka and Magendie (red cross at red arrow) during development, caused ventricular dilation, increasing greatly the surface of the ventricular wall. Venous structures (inset) on the ventricular wall of the fourth (IV) and lateral ventricles (LV) were found in the patient with Dandy Walker. They may fulfil the role of the Pacchionian granulations in the normal brain and facilitate CSF drainage into the venous system. The prominent subependymal veins and the enlarged internal cerebral veins and straight sinus (sinus rectus) may substitute in part for the small superior sagittal sinus in this patient (see Fig 2a) and perhaps in others with giant hydrocephalus (see Fig 1d). The colour code assigned to the various fluids is displayed in Fig S3a.

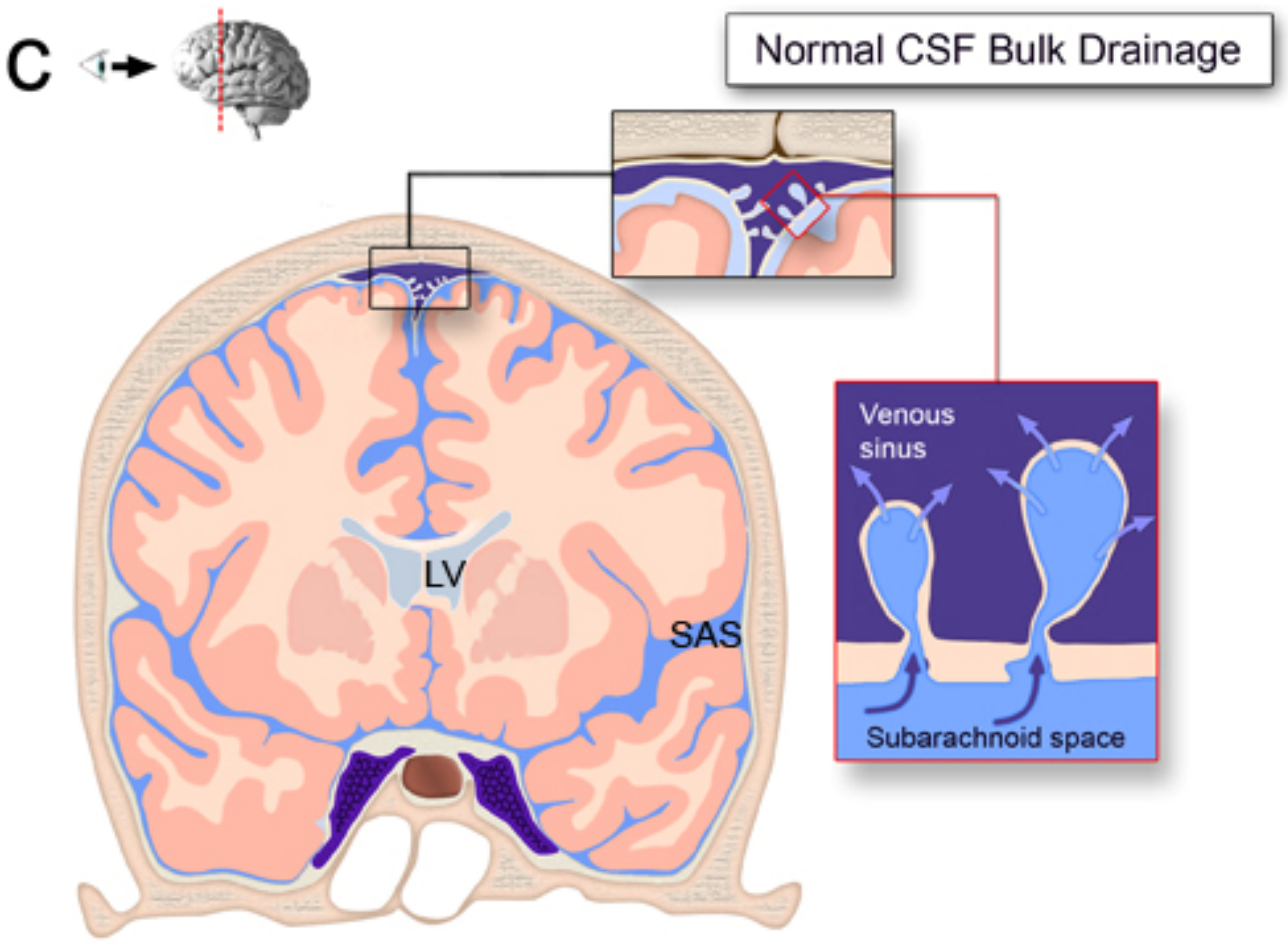

S3c. Normal CSF circulation *(coronal section at a pre-thalamic level).* Compare with Fig S3a. Cerebrospinal fluid (CSF) is normally secreted by the choroid plexus, mostly in the lateral ventricles (LV). From the ventricles, it drains into the subarachnoid space (SAS) around the brain. In the SAS the CSF moves toward the large venous sinuses located in the fibrous layer that separates the brain from the bone of the skull (inset). A valve-like system, constituted by the Pacchionian granulations (insets), separates the CSF from the blood in the venous sinuses, while permitting CSF to drain into the venous system. The arrows in the inset indicate the direction of flow, from the subarachnoid space into the venous sinus. The colour code assigned to the various fluids is displayed in Fig S3a.

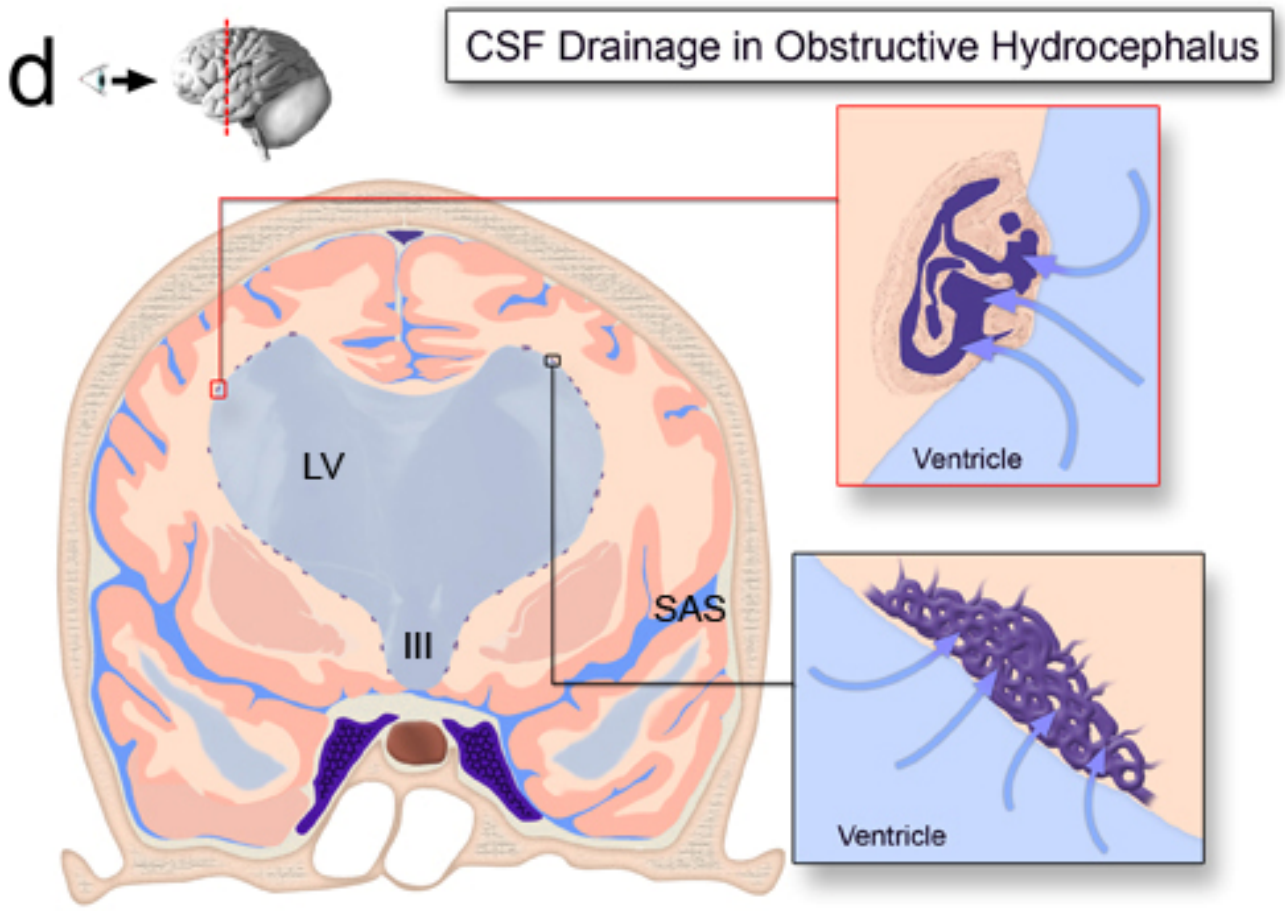

S3d. Hypothesized CSF flow in subjects with compensated giant hydrocephalus *(coronal section at a pre-thalamic level).* This view allows for a clear visualization of the position of the unusual vascular structures found in the ventricular wall of the patient with Dandy-Walker syndrome (insets). Compare with Figs. 3, 4 and S3d. Obstruction of ventricular outflow causes ventricular dilation, increasing greatly the surface of the ventricular wall. The venous structures on the ventricular wall may work in chronic hydrocephalus as the Pacchionian granulations in the normal brain and facilitate CSF drainage into the venous system. The colour code assigned to the various fluids is displayed in Fig S3a.

Supplemental Discussion

Some recent views on the genesis of hydrocephalus and on CSF circulation, particularly from data in experimental animals and in humans with communicating hydrocephalus, have challenged the traditional concept of CSF bulk flow depicted on Fig S3.[7, 8] However, in the adult human and even in the child, the flow from the ventricles to the subarachnoid space is critical, as gauged by the dire clinical consequences and the tissue damage derived from acquired obstruction of the CSF pathways.[9, 10] CSF flow, facilitated in this individual with giant hydrocephalus by venular ventricular-wall structures, has important roles for the homeostasis of the brain, devoid of a lymphatic draining system. Proteins and other waste products move normally from the extracellular space of the brain into the CSF, which deposits them into the venous system (toilet function of the CSF).[9] If not properly cleared, these substances may interfere with brain function. In acute experimental hydrocephalus and in poorly compensated hydrocephalic children, there are periventricular fluid collections, likely representing stagnant extracellular fluid into which substances slowly diffuse from the CSF.[11] The correspondingly increased amount of water causes hyperintensity on T2-weighted MRI, not present in the MRI of individuals well adapted to giant hydrocephalus (Fig 1c). The vessels we describe are suitably formed and placed to drain the stagnant fluid. White matter oedema was not present in the 48-year-old man with a Dandy Walker malformation. These findings tend to suggest that the draining mechanism we describe may contribute to spare the important toilet function of the CSF and therefore minimize the impact of giant hydrocephalus on neurological function, including cognition.

References for the Online Supplement

1. World Medical Association. World Medical Association declaration of Helsinki. Ethical principles for medical research involving human subjects. http://www.wma.net/e/policy/pdf/17c.pdf. Accessed 8 July 2008, 2008.

2. Reichenbach JR, Venkatesan R, Schillinger DJ, Kido DK, Haacke EM. Small vessels in the human brain: MR venography with deoxyhemoglobin as an intrinsic contrast agent. *Radiology.* 1997;204(1):272-277.

3. Wang J, Alsop DC, Li L, et al. Comparison of quantitative perfusion imaging using arterial spin labeling at 1.5 and 4.0 Tesla. *Magn Reson Med.* 2002;48(2):242-254.

4. Shattuck DW, Leahy RM. BrainSuite: an automated cortical surface identification tool. *Med Image Anal.* 2002;6(2):129-142.

5. Wang J, Zhang Y, Wolf RL, Roc AC, Alsop DC, Detre JA. Amplitude-modulated continuous arterial spin-labeling 3.0-T perfusion MR imaging with a single coil: feasibility study. *Radiology.* 2005;235(1):218-228.

6. Frackowiak RS, Lenzi GL, Jones T, Heather JD. Quantitative measurement of regional cerebral blood flow and oxygen metabolism in man using 15O and positron emission tomography: theory, procedure, and normal values. *J Comput Assist Tomogr.* 1980;4(6):727-736.

7. Bateman GA. Extending the hydrodynamic hypothesis in chronic hydrocephalus. *Neurosurg Rev.* 2005;28(4):333-334.

8. Greitz D. Radiological assessment of hydrocephalus: new theories and implications for therapy. *Neurosurg Rev.* 2004;27(3):145-165; discussion 166-147.

9. Del Bigio MR. Cellular damage and prevention in childhood hydrocephalus. *Brain Pathol.* 2004;14(3):317-324.

10. Oi S, Di Rocco C. Proposal of "evolution theory in cerebrospinal fluid dynamics" and minor pathway hydrocephalus in developing immature brain. *Childs Nerv Syst.* 2006;22(7):662-669.

11. Del Bigio MR. Neuropathological changes caused by hydrocephalus. *Acta Neuropathol (Berl).* 1993;85(6):573-585.